Research Journal of Applied Sciences, Engineering and Technology 5(6): 1864-1875, 2013
DOI:10.19026/rjaset.5.4723
ISSN: 2040-7459; e-ISSN: 2040-7467

Submitted: April 23, 2012 Accepted: June 08, 2012 Published: February 21, 2013

Research Article

Combined Effects of Hall Currents and Rotation on Steady Hydromagnetic Couette Flow

Bhaskar Chandra Sarkar, Sanatan Das and Rabindra Nath Jana
Department of Applied Mathematics, Vidyasagar University, Midnapore, 721102, India

Abstract: We study a steady hydromagnetic Couette flow of a viscous incompressible electrically conducting fluid in a rotating system between two infinitely long parallel plates in the presence of a uniform transverse magnetic field on taking Hall Current into account. The governing equations describing the flow are solved analytically. It is observed that the Hall currents accelerate the primary velocity whereas they retard the secondary velocity. The induced magnetic field is significantly affected by the Hall currents. An increase in Hall currents leads to fall in the fluid temperature. The heat transfer characteristics have also been studied. The rate of heat transfer at the lower plate decreases whereas the rate of heat transfer at the upper plate increases with an increase in Hall parameter. The asymptotic behavior of the solutions are discussed for small and large values of magnetic parameter and rotation parameter. It is interesting to note that either for strong magnetic field or for large rotation there exists a single-deck boundary layer in the region near the stationary plate. The thickness of this boundary layer first decreases, reaches a minimum and then increases with an increase in Hall parameter.

Keywords: Couette flow, eckert number, hall currents, heat transfer, MHD, rotation parameter, steady flow

INTRODUCTION

Couette flows find widespread applications in geophysics, planetary sciences and also in many areas of industrial engineering. For many decades engineers have studied such flows with and without rotation and also for both the steady and unsteady cases. In the ionized gases, the current is not proportional to the applied potential except when the electric field is very weak. However, in the presence of strong electric field, the electrical conductivity is affected by the magnetic field. Consequently, the conductivity parallel to the electric field is reduced. Hence, the current is induced in the direction normal to both the electric and magnetic fields. This phenomenon well known in literature is known as the *Hall effects*. Due to these Hall Currents the electrical conductivity of the fluid becomes anisotropic and this causes secondary flow in magnetohydrodynamic primary flows. Hall Currents are of great importance in many astrophysical problems, Hall accelerator and flight MHD as well as flows of plasma in a MHD power generator. The study of the interaction of the Coriolis force with the electromagnetic force is also important. In particular, rotating MHD flows with heat transfer is one of the important current topics because of its applications in thermofluid transport modeling in magnetic geosystems and in some astrophysical problems. Hartmann and Lazarus (1937) have investigated the influence of a transverse uniform magnetic field on the flow of a viscous incompressible electrically conducting fluid between two infinite parallel stationary and insulating plates. The problem is extended in numerous ways. Closed form solutions for the velocity fields have been obtained by Tao (1960), Alpher (1961), Sutton and Sherman (1965) and Cramer and Pai (1973) under different physical effects. In the above mentioned cases the Hall term was ignored in applying Ohm's law as it has no marked effect for small and moderate values of the magnetic field. However, the current trend for the application of magnetohydrodynamics is towards a strong magnetic field so that the influence of electromagnetic force is noticeable. Under these conditions, the Hall Currents are important and they have a significant effect on the magnitude and direction of the current density and consequently on the magnetic force. Hall effects on hydromagnetic Couette flow and heat transfer have been studied by Gupta (1972). Soundalgekar *et al.* (1974) have obtained the Hall effects on generalized MHD Couette flow with heat transfer. MHD Couette flow and heat transfer in a rotating system have been studied by Jana *et al.* (1977). Seth and Maiti (1982), Mandal *et al.* (1982) and Seth *et al.* (1982, 1985, 2009) have studied MHD Couette flow of a rotating system in the presence of a uniform transverse magnetic field considering different aspects of the problem. Ghosh (2002) has studied the effects of Hall current on MHD Couette flow in a rotating system

Corresponding Author: Bhaskar Chandra Sarkar, Department of Applied Mathematics, Vidyasagar University, Midnapore, 721102, India

with arbitrary magnetic field. Das *et al.* (2008) have investigated Couette flow in a viscous incompressible fluid in a rotating system in the absence of magnetic field. Seth *et al.* (2009) have discussed MHD Couette flow of a viscous incompressible electrically conducting fluid in the presence of a uniform magnetic field neglecting induced magnetic field. Hall effects on MHD Couette flow between two infinite horizontal parallel porous plates in a rotating system under the boundary layer approximations have been studied by Das *et al.* (2011). Seth *et al.* (2011) have obtained steady MHD Couette flow of a viscous incompressible electrically conducting fluid in a rotating system.

In the present study, we have studied the effects of Hall Current and rotation on the MHD Couette flow of a viscous incompressible electrically conducting fluid in a rotating system in the presence of a uniform transverse magnetic field on taking induced magnetic field into account. The lower plate is perfectly conducting whereas the upper plate is non-conducting. The upper plate is moving with a constant velocity U_0 while the lower plate is kept stationary. It is found that both the primary velocity u_1 and the secondary velocity v_1 decrease with an increase in magnetic parameter M^2. It is also found that both the velocities increase with an increase in rotation parameter K^2. It is seen that the primary velocity u_1 increases whereas the secondary velocity v_1 decreases with an increase in Hall parameter m. It is observed that both the primary and secondary induced magnetic field components b_x and b_y decrease with an increase in magnetic parameter M^2 whereas they increase with an increase in rotation parameter K^2. It is also seen that the primary induced magnetic field component b_x decreases while the secondary induced magnetic field component b_y increases with an increase in Hall parameter m. It is found that the shear stress at the lower plate due to the primary flow increases while the shear stress at the lower plate due to the secondary flow decreases with an increase in Hall parameter. The heat transfer characteristics have also been studied on taking viscous and Joule dissipations into account. The rate of heat transfer at the lower plate decreases while the rate of heat transfer at the upper plate increases with an increase in Hall parameter.

Formulation of the problem and its solutions: The basic equations of magnetohydrodynamics for steady flow are:

$$(\vec{q}\cdot\nabla)\vec{q} + 2\Omega\hat{k}\times\vec{q} = -\frac{1}{\rho}\nabla p + \nu\nabla^2\vec{q} + \frac{1}{\rho}\vec{j}\times\vec{B}, \tag{1}$$

$$\nabla\cdot\vec{q} = 0, \tag{2}$$

$$\nabla\times\vec{B} = \mu_e\vec{j}, \tag{3}$$

$$\nabla\times\vec{E} = 0 \quad \text{(for steady flow)}, \tag{4}$$

$$\nabla\cdot\vec{B} = 0 \tag{5}$$

together with generalized Ohm's law taking Hall current into account is (Cowling, 1957):

$$\vec{j} + \frac{\omega_e\tau_e}{B_0}\left(\vec{j}\times\vec{B}\right) = \sigma\left(\vec{E} + \vec{q}\times\vec{B}\right), \tag{6}$$

where, $\vec{q}$, $\vec{B}$, $\vec{E}$, $\vec{j}$, Ω are respectively the velocity vector, the magnetic field vector, the electric field vector, the current density vector and angular velocity. Also σ, ν, μ_e, ρ, p, B_0, ω_e and τ_e are the electric conductivity, kinematic coefficient of viscosity, magnetic permeability, fluid density, modified fluid pressure including centrifugal force, applied magnetic field, cyclotron frequency and electron collision time respectively. In writing the Eq. (6), the ion-slip and the thermoelectric effects as well as the electron pressure gradient are neglected.

Consider the viscous incompressible electrically conducting fluid bounded by two infinite horizontal parallel plates separated by a distance d. Choose a Cartesian co-ordinates system with x-axis along the lower stationary plate in the direction of the flow, the z-axis is normal to the plates and the y-axis is perpendicular to xz-plane (Fig. 1). The lower plate is perfectly conducting whereas the upper plate is non-conducting. The upper plate is moving with a uniform velocity U_0 while the lower plate is held at rest. The plate and the fluid rotate in unison with uniform angular velocity Ω about an axis perpendicular to the plates. A uniform magnetic field B_0 is applied in the positive z-direction. Since the plates are infinitely long, all physical variables, except pressure, depend on z only.

The equation of continuity $\nabla\cdot\vec{q} = 0$ with no-slip condition at the plates gives w = 0 everywhere in the flow where $\vec{q} \equiv (u, v, w)$. The solenoidal relation $\nabla\cdot\vec{B} = 0$ gives B_z = constant = B_0 everywhere in the flow where $\vec{B} \equiv (B_x, B_y, B_0)$.

The momentum equations for the fully developed steady flow are:

$$-2\Omega v = -\frac{1}{\rho}\frac{\partial p}{\partial x} + \nu\frac{d^2u}{dz^2} + \frac{B_0}{\rho\mu_e}\frac{dB_x}{dz}, \tag{7}$$

$$2\Omega u = -\frac{1}{\rho}\frac{\partial p}{\partial y} + \nu\frac{d^2v}{dz^2} + \frac{B_0}{\rho\mu_e}\frac{dB_y}{dz}, \tag{8}$$

$$0 = \frac{1}{\rho}\frac{\partial p}{\partial z} + \frac{1}{2\rho\mu_e}\left(\frac{dB_x^2}{dz} + \frac{dB_y^2}{dz}\right), \tag{9}$$

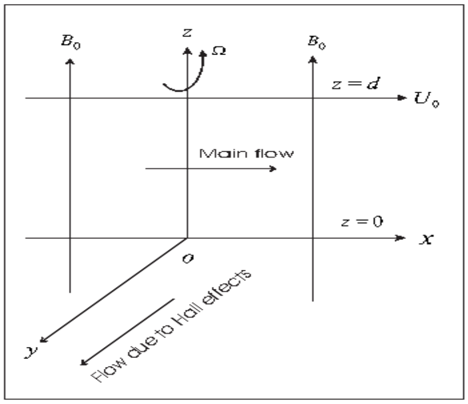

Fig. 1: Geometry of the problem

Eliminating $\vec{E}$ from Eq. (4) and (6), we have the x- and y-components of the magnetic induction equations as:

$$\frac{d^2 B_x}{dz^2} + m\frac{d^2 B_y}{dz^2} + \sigma\mu_e B_0 \frac{du}{dz} = 0, \tag{10}$$

$$\frac{d^2 B_y}{dz^2} - m\frac{d^2 B_x}{dz^2} + \sigma\mu_e B_0 \frac{dv}{dz} = 0, \tag{11}$$

where m = $\omega_e \ \tau_e$ is the Hall parameter.

The boundary conditions for the velocities and the magnetic fields are:

$$u = 0,\ v = 0,\ \ \frac{dB_x}{dz} = \frac{dB_y}{dz} = 0,\ \text{ at }\ \ z = 0;$$

$$u = U_0, v = 0, B_x = 0,\ B_y = 0,\ \text{ at }\ \ z = d. \tag{12}$$

On the use of the boundary condition at z = d, we have from Eq. (7) and (8):

$$-\frac{1}{\rho}\frac{\partial p}{\partial x} = 0 \ \text{ and }\ -\frac{1}{\rho}\frac{\partial p}{\partial y} = 2\Omega U_0. \tag{13}$$

Using (13), Eq. (7) and (8) become:

$$-2\Omega v = \nu\frac{d^2 u}{dz^2} + \frac{B_0}{\rho\mu_e}\frac{dB_x}{dz}, \tag{14}$$

$$2\Omega(u - U_0) = \nu\frac{d^2 v}{dz^2} + \frac{B_0}{\rho\mu_e}\frac{dB_y}{dz}. \tag{15}$$

Introducing the non-dimensional variables:

$$\eta = \frac{z}{d},\ (u_1, v_1) = \frac{(u,v)}{U_0},\ (b_x, b_y) = \frac{(B_x, B_y)}{\sigma\mu_e B_0 U_0 d}, \tag{16}$$

Equations (14), (15), (10) and (11) become:

$$-2K^2 v_1 = \frac{d^2 u_1}{d\eta^2} + M^2\frac{db_x}{d\eta}, \tag{17}$$

$$2K^2(u_1 - 1) = \frac{d^2 v_1}{d\eta^2} + M^2\frac{db_y}{d\eta}, \tag{18}$$

$$\frac{d^2 b_x}{d\eta^2} + m\frac{d^2 b_y}{d\eta^2} + \frac{du_1}{d\eta} = 0, \tag{19}$$

$$\frac{d^2 b_y}{d\eta^2} - m\frac{d^2 b_x}{d\eta^2} + \frac{dv_1}{d\eta} = 0, \tag{20}$$

where, $M^2 = \frac{\sigma B_0^2 d^2}{\rho\nu}$ is the magnetic parameter and $K^2 = \frac{\Omega d^2}{\nu}$ the rotation parameter. Combining Eq. (17), (18), (19) and (20), we get:

$$\frac{d^2 F}{d\eta^2} + M^2\frac{db}{d\eta} = 2iK^2(F - 1), \tag{21}$$

$$(1 - im)\frac{d^2 b}{d\eta^2} + \frac{dF}{d\eta} = 0, \tag{22}$$

where,

$$F = u_1 + iv_1,\ b = b_x + ib_y \ \text{ and }\ i = \sqrt{-1}. \tag{23}$$

The corresponding boundary conditions for $F(\eta)$ and $b(\eta)$ are:

$$F = 0 \ \text{ at }\ \eta = 0 \ \text{ and }\ F = 1 \ \text{ at }\ \eta = 1,$$

$$\frac{db}{d\eta} = 0 \ \text{ at }\ \eta = 0 \ \text{ and }\ b = 0 \ \text{ at }\ \eta = 1. \tag{24}$$

The solutions of the Eq. (21) and (22) subject to the boundary conditions (24) are:

$$F(\eta) = \frac{\sinh\lambda\eta}{\sinh\lambda} + c_1\left[\frac{\sinh\lambda(1-\eta)}{\sinh\lambda} + \frac{\sinh\lambda\eta}{\sinh\lambda} - 1\right], \tag{25}$$

$$b(\eta)=\frac{1}{(1-im)}\left[\frac{\cosh\lambda-\cosh\lambda\eta}{\lambda\sinh\lambda}+c_1\left(\eta-1\right.\right.$$

$$\left.\left.+\frac{\cosh\lambda-\cosh\lambda\eta}{\lambda\sinh\lambda}+\frac{\cosh\lambda(1-\eta)-1}{\lambda\sinh\lambda}\right)\right]. \tag{26}$$

where,

$$\lambda=\alpha+i\beta,\ c_1=-\frac{2iK^2}{\lambda^2},$$

$$\alpha,\beta=\frac{1}{\sqrt{2}}\left[\left\{\left(\frac{M^2}{1+m^2}\right)^2+\left(2K^2+\frac{mM^2}{1+m^2}\right)^2\right\}^{\frac{1}{2}}\pm\left(\frac{M^2}{1+m^2}\right)\right]^{\frac{1}{2}}. \tag{27}$$

On separating into real and imaginary parts one can easily obtain the velocity components u_1 and v_1 from Eq. (25) and the induced magnetic field components b_x and b_y from Eq. (26). If m = 0, then the Eq. (25) and (26) are identical with the Eq. (23) and (24) of Seth *et al*. (2011).

RESULTS AND DISCUSSION

We have plotted the non-dimensional primary and secondary velocities u_1 and v_1 against η for several values of magnetic parameter M^2, rotation parameter K^2 and Hall parameter m in Fig. 2 to 4. Figure 2 displays that both the primary velocity u_1 and the secondary velocity v_1 decrease with an increase in magnetic parameter M^2 which implies that magnetic field has retarding influence on both the primary and the secondary flow. Figure 3 shows that the primary velocity u_1 increases with an increase in rotation parameter K^2 whereas the secondary velocity v_1 increases in the vicinity of the lower plate and decreases away from the lower plate with an increase in rotation parameter K^2. The rotation parameter K^2 defines the relative magnitude of the Coriolis force and the viscous force in the regime, therefore it is clear that the high magnitude Coriolis forces are counter-productive for the primary flow. It is observed from Fig. 4 that the primary velocity u_1 increases whereas the secondary velocity v_1 decreases with an increase in Hall parameter m. This implies that Hall currents accelerate the primary flow and retard the secondary flow. Also we have presented the non-dimensional primary and secondary induced magnetic field components b_x and b_y against η for several values of magnetic parameter M^2, rotation parameter K^2 and Hall parameter *m* in Fig. 5 to 7. It is revealed from Fig. 5 that both the induced

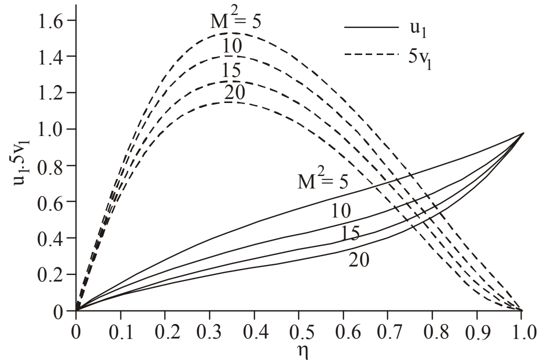

Fig. 2: Primary and secondary velocities for M^2 when m = 0.5 and K^2 = 5

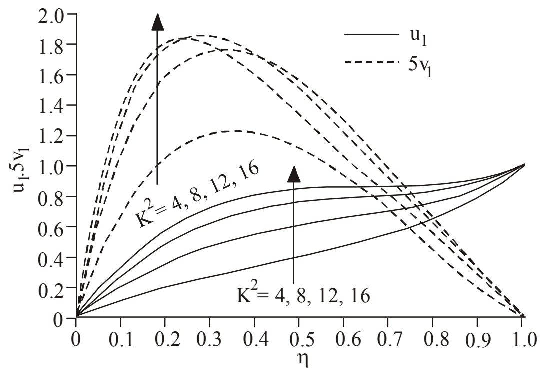

Fig. 3: Primary and secondary velocities for K^2 when M^2 = 10 and m = 0.5

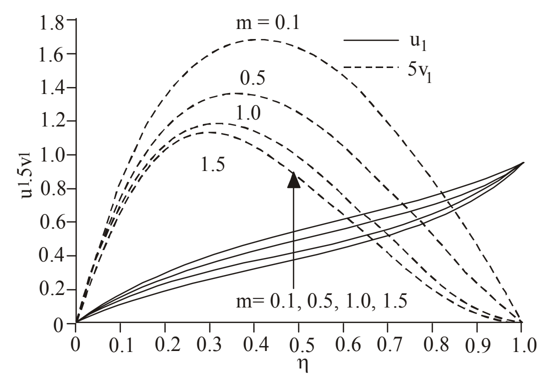

Fig. 4: Primary and secondary velocities for m when M^2 = 10 and K^2 = 5

magnetic field components b_x and b_y decrease with an increase in magnetic parameter M^2 which means that magnetic field has a trendeny to reduce the primary and the secondary induced magnetic fields in the presence of Hall Currents. It is seen from Fig. 6 that both the primary and the secondary induced magnetic field

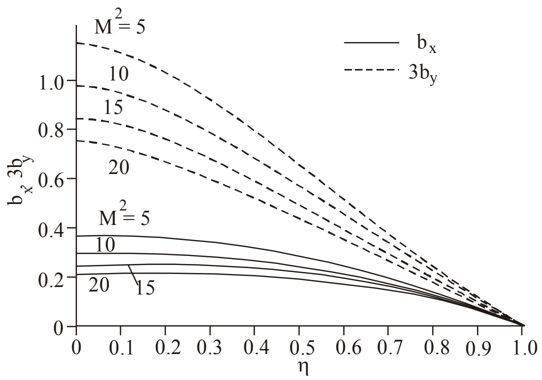

Fig. 5: Primary and secondary induced magnetic fields for M^2 when m = 0.5 and $K^2 = 5$

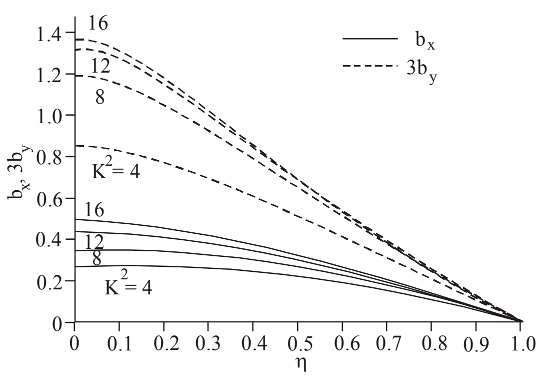

Fig. 6: Primary and secondary induced magnetic fields for K^2 when $M^2 = 10$ and m = 0.5

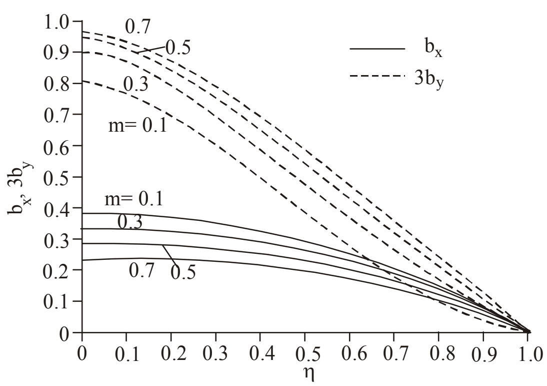

Fig. 7: Primary and secondary induced magnetic fields for m when $M^2 = 10$ and $K^2 = 5$

components b_x and b_y increases with an increase in rotation parameter K^2. It indicates that rotation tends to enhance both the primary and the secondary induced magnetic field components. Figure 7 reveals that with an increase in Hall parameter m the induced magnetic field component b_x decreases whereas b_y increases which means that Hall Currents tend to reduce the primary induced magnetic field component b_x whereas Hall Currents tend to enhance the secondary induced magnetic field component b_y.

The non-dimensional shear stresses due to the primary and the secondary flows at the lower plate ($\eta = 0$) and the upper plate ($\eta = 1$) are, respectively:

$$\tau_{x_0} + i\tau_{y_0} = \left(\frac{dF}{d\eta}\right)_{\eta=0} = \frac{1}{\lambda \sinh \lambda}\left[\frac{M^2}{1-im} + 2iK^2 \cosh \lambda\right], \tag{28}$$

$$\tau_{x_1} + i\tau_{y_1} = \left(\frac{dF}{d\eta}\right)_{\eta=1} = \frac{1}{\lambda \sinh \lambda}\left[\frac{M^2}{1-im}\cosh \lambda + 2iK^2\right], \tag{29}$$

where λ is given by (27).

Numerical results of the shear stresses at the plates ($\eta = 0$) and ($\eta = 1$) are depicted in Fig. 8 to 11 against m for various values of magnetic parameter M^2 and rotation parameter K^2. Figure 8 shows that at the lower plate ($\eta = 0$) both the shear stress τ_{x_0} due to the primary flow and the shear stress τ_{y_0} due to the secondary flow decrease with an increase in magnetic parameter M^2. This implies that the magnetic field has tendency to reduce the primary shear stress as well as the secondary shear stress at the lower plate. It is seen from Fig. 9 that at the lower plate ($\eta = 0$) both the shear stresses τ_{x_0} and τ_{y_0} increase with an increase in rotation parameter K^2. This means that rotation has tendency to enhance the primary as well as the secondary shear stresses at the lower plate. Further, it is observed from Fig. 10 that at the upper plate ($\eta = 1$) both the shear stress τ_{x_1} due to the primary flow and the shear stress τ_{y_1} due to the secondary flow increase with an increase in magnetic parameter M^2 which implies that the magnetic field has tendency to enhance the primary shear stress as well as the secondary shear stress at the upper plate. It is seen from Fig. 11 that at the upper plate ($\eta = 1$) both the shear stresses τ_{x_1} and τ_{y_1} decrease with an increase in rotation parameter K^2 which implies that rotation has tendency to reduce the primary as well as the secondary shear stresses at the upper plate. Further it is observed from Fig. 8 and 9 that τ_{x_0} increases and τ_{y_0} decreases with an increase in Hall parameter m. Figure 10 and 11 show that τ_{x_1} decreases and τ_{y_1} increases with an increase in Hall parameter m. Thus, Hall currents have tendency to enhance the primary shear stress and to reduce the secondary shear stress at the lower plate whereas Hall currents have tendency to reduce the

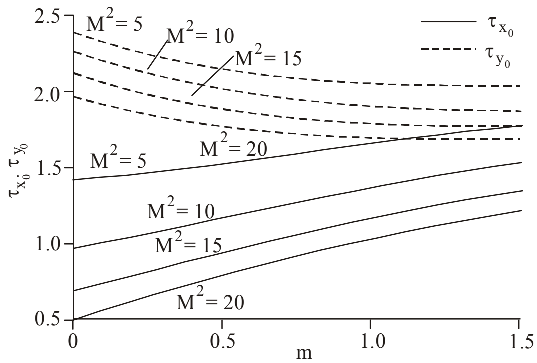

Fig. 8: Shear stresses τ_{x_0} and τ_{y_0} for M^2 when $K^2 = 5$

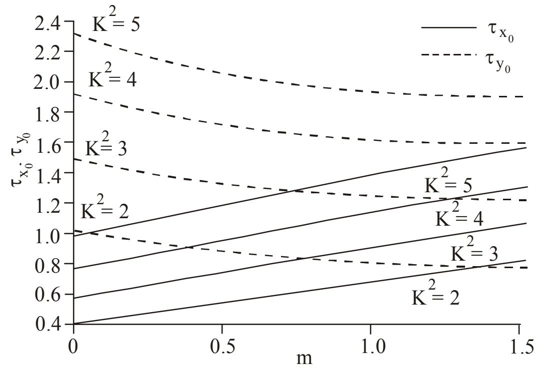

Fig. 9: Shear stresses τ_{x_0} and τ_{y_0} for K^2 when $M^2 = 10$

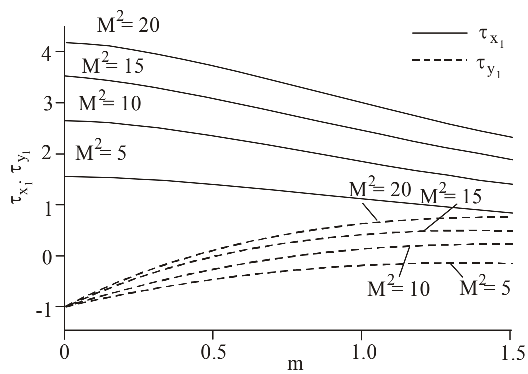

Fig. 10: Shear stresses τ_{x_1} and τ_{y_1} for M^2 when $K^2 = 5$

primary shear stress and to enhance the secondary shear stress at the upper plate.

We shall now discuss the asymptotic behavior of the solutions (25) and (26) for small and large values of M^2 and K^2:

Case I: When M^2<<1 and K^2<<1. In this case, the Eq. (21) and (22) become:

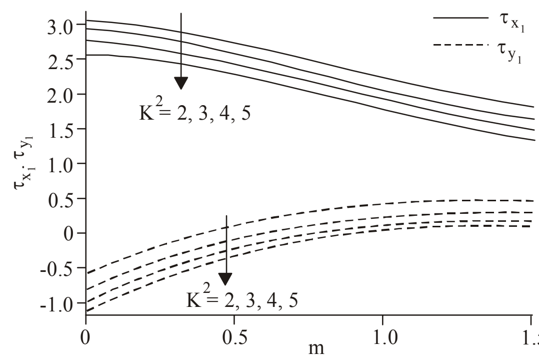

Fig. 11: Shear stresses τ_{x_1} and τ_{y_1} for K^2 when $M^2 = 10$

$$u_1 = \eta - \frac{1}{6}\frac{M^2}{1+m^2}\eta(1-\eta^2) + ..., \tag{30}$$

$$v_1 = \frac{K^3}{3}\eta(2-3\eta+\eta^2) - \frac{1}{6}\frac{mM^2}{1+m^2}\eta(1-\eta^2) + ..., \tag{31}$$

$$b_x = \frac{1}{1+m^2}\left[\frac{1}{2}(1-\eta^2) - \frac{M^2}{24}\frac{1}{1+m^2}(1-2\eta^2+\eta^4) - \frac{mK^2}{12}(1-4\eta^2+4\eta^3-\eta^4) + ...\right], \tag{32}$$

$$b_y = \frac{1}{1+m^2}\left[m\left\{\frac{1}{2}(1-\eta^2) - \frac{M^2}{12}\frac{1}{1+m^2}(1-2\eta^2+\eta^4)\right\} + \frac{K^2}{12}(1-4\eta^2+4\eta^3-\eta^4) + ...\right]. \tag{33}$$

It is observed from Eq. (30) to (33) that for small values of K^2 and M^2, the primary velocity is independent of the rotation parameter K^2 but depend on magnetic parameter and Hall parameter. On the other hand, secondary velocity, primary and secondary induced magnetic field components depend on the rotation parameter as well as magnetic parameter and Hall parameter.

Case II: When K^2>>1 and $M^2 \approx O$ (1). For the boundary layer flow adjacent to the upper plate η = 1, we introduce ξ = 1 - η and then the Eq. (21) and (22) give:

$$u_1 = 1 - \frac{M^2}{2K^2(1+m^2)}\left[m - e^{-\alpha_1\xi}(m\cos\beta_1\xi - \sin\beta_1\xi)\right], \tag{34}$$

$$v_1 = \frac{M^2}{2K^2(1+m^2)}\left[1 - e^{-\alpha_1\xi}(\cos\beta_1\xi + m\sin\beta_1\xi)\right], \quad (35)$$

$$b_x = \frac{\xi}{1+m^2}\left[1 - \frac{mM^2}{K^2(1+m^2)}\right] - \frac{M^2}{4K^3(1+m^2)^2}\left[1 - 2m\right.$$

$$\left. - e^{-\alpha_1\xi}\left\{(1-2m)\cos\beta_1\xi + (1+2m)\sin\beta_1\xi\right\}\right], \quad (36)$$

$$b_y = \frac{M^2}{2K^2}\frac{\xi}{(1+m^2)^2} - \frac{M^2}{4K^3(1+m^2)^2}\left[1 + 2m\right.$$

$$\left. - e^{-\alpha_1\xi}\left\{(1+2m)\cos\beta_1\xi - (1-2m)\sin\beta_1\xi\right\}\right], \quad (37)$$

where,

$$\alpha_1, \beta_1 = K\left[1 \pm \frac{(1\pm m)M^2}{4K^2(1+m^2)}\right]. \quad (38)$$

It is seen from the Eq. (34) and (35) that there exists a single-deck boundary layer of thickness of the order $O(1/\alpha_1)$ where α_1 is given by (38). It is observed that the thickness of this boundary layer decreases with an increase in magnetic parameter M^2. Figure 12 shows that the boundary layer thickness first decreases, reaches a minimum and then increases with an increase in Hall parameter m while the thickness of this boundary layer has oscillatory in nature with an increase in rotation parameter K^2.

It is seen that the exponential terms in (34) to (37) damp out quickly as ξ increases. When $\xi \geq 1/\alpha_1$ i.e., outside the boundary layer region, the velocities and induced magnetic field components become:

$$u_1 = 1 - \frac{mM^2}{2K^2(1+m^2)}, \quad v_1 = \frac{M^2}{2K^2(1+m^2)}, \quad (39)$$

$$b_x = \frac{\xi}{1+m^2}\left[1 - \frac{mM^2}{K^2(1+m^2)}\right] - \frac{M^2}{4K^3(1+m^2)^2}(1-2m),$$

$$b_y = \frac{M^2}{2K^2}\frac{\xi}{(1+m^2)^2} - \frac{M^2}{4K^3(1+m^2)^2}(1+2m). \quad (40)$$

Case III: When $M^2 >> 1$ and $K^2 \approx O(1)$. In this case, the Eq. (21) and (22) give:

$$u_1 = \frac{2mK^2}{M^2} + e^{-\alpha_2\xi}\left[\left(1 + \frac{3}{4}m^2 + \frac{mK^2}{M^2}\right)\cos\beta_2\xi\right.$$

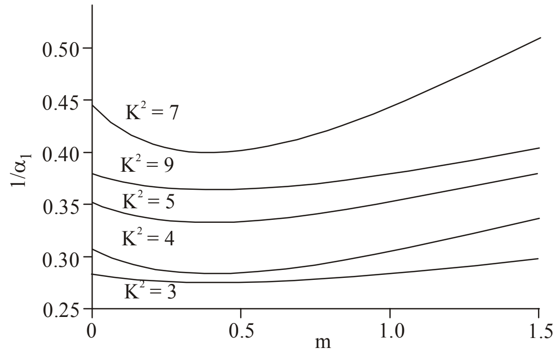

Fig. 12: Boundary layer thickness when $M^2 = 10$

$$\left. - \frac{2K^2}{M^2}\sin\beta_2\xi\right], \quad (41)$$

$$v_1 = \frac{2K^2}{M^2} - e^{-\alpha_2\xi}\left[\frac{2K^2}{M^2}\cos\beta_2\xi + \left(1 + \frac{3}{4}m^2 + \frac{mK^2}{M^2}\right)\sin\beta_2\xi\right], \quad (42)$$

$$b_x = \frac{1}{M\sqrt{1+m^2}}\left[1 + \frac{1}{2}m^2 - e^{-\alpha_2\xi}\left\{\left(1 + \frac{1}{2}m^2\right)\cos\beta_2\xi\right.\right.$$

$$\left.\left. + \left(\frac{1}{2}m - \frac{3K^2}{M^2}\right)\sin\beta_2\xi\right\}\right], \quad (43)$$

$$b_y = \frac{2K^2\xi}{M^2} + \frac{1}{M\sqrt{1+m^2}}\left[\frac{1}{2}m - \frac{3K^2}{M^2}\right.$$

$$\left. - e^{-\alpha_2\xi}\left\{\left(\frac{1}{2}m - \frac{3K^2}{M^2}\right)\cos\beta_2\xi - \left(1 + \frac{1}{2}m^2\right)\sin\beta_2\xi\right\}\right], \quad (44)$$

where,

$$\alpha_2 = \frac{M}{\sqrt{1+m^2}}, \quad \beta_2 = \left(\frac{K^2}{M}\sqrt{1+m^2} + \frac{mM}{2\sqrt{1+m^2}}\right). \quad (45)$$

It is seen from the Eq. (41) and (42) that there exists a single-deck boundary layer of thickness of the order $O(1/\alpha_2)$ where α_2 is given by (45). It is revealed that the thickness of this boundary layer increases with increase in Hall parameter m but it decreases with an increase in magnetic parameter M^2. It is interesting to note that for large magnetic parameter, that is, for strong magnetic field the boundary layer thickness is independent of rotation parameter K^2.

It is seen that the exponential terms in (41) to (44) damp out quickly as ξ increases. When $\xi \geq 1/\alpha_2$ i.e., outside the boundary layer region, the velocities and induced magnetic field components reduce to:

$$u_1 = \frac{2mK^2}{M^2},\ v_1 = \frac{2K^2}{M^2}, \tag{46}$$

$$b_x = \frac{1+\frac{1}{2}m^2}{M\sqrt{1+m^2}},\ b_y = \frac{2K^2\xi}{M^2} + \frac{\frac{1}{2}m - \frac{3K^2}{M^2}}{M\sqrt{1+m^2}}. \tag{47}$$

Heat transfer: The energy equation for the fully developed flow including the viscous and Joule dissipations is:

$$k\frac{d^2T}{dz^2} + \mu\left[\left(\frac{du}{dz}\right)^2 + \left(\frac{dv}{dz}\right)^2\right]$$

$$+\frac{1}{\sigma\mu_e^2}\left[\left(\frac{dB_x}{dz}\right)^2 + \left(\frac{dB_y}{dz}\right)^2\right] = 0, \tag{48}$$

where,
k : The thermal conductivity
μ : The dynamic viscosity

The temperature boundary conditions are:

$$T = T_0 \ \text{ at } \ z = 0,\ T = T_1 \ \text{ at } \ z = d, \tag{49}$$

where, T_0 and $T_1(T_1>T_0)$ denote the uniform temperature of the plates at z = 0 and z = d respectively. Introducing:

$$\theta = \frac{T - T_0}{T_1 - T_0}, \tag{50}$$

and on the use of (16) and (23), the energy Eq. (48) can be written in a dimensionless form as:

$$\frac{d^2\theta}{d\eta^2} + Pr\,Ec\left[\left(\frac{du_1}{d\eta}\right)^2 + \left(\frac{dv_1}{d\eta}\right)^2\right.$$

$$\left. +M^2\left\{\left(\frac{db_x}{d\eta}\right)^2 + \left(\frac{db_y}{d\eta}\right)^2\right\}\right] = 0, \tag{51}$$

where, $\Pr = \frac{\mu C_p}{k}$ is the Prandtl number, $Ec = \frac{U_0^2}{C_{p(T_1 - T_0)}}$ the Eckert number and C_P the specific heat at constant pressure .

The corresponding temperature boundary conditions for θ(η) become:

$$\theta(0) = 0 \ \text{ and } \ \theta(1) = 1. \tag{52}$$

Using Eq. (25) and (26), the solution of Eq. (51) subject to the boundary conditions (52) is:

$$\theta(\eta) = \eta + PrEc\left[(Y - X)\eta + X - \left\{\frac{P}{8\alpha^2}(A\bar{A} + B\bar{B})\cosh 2\alpha\eta\right.\right.$$

$$-\frac{Q}{8\beta^2}(A\bar{A} - B\bar{B})\cos 2\beta\eta$$

$$+\frac{P}{8\alpha^2}(A\bar{B} + B\bar{A})\sinh 2\alpha\eta - \frac{iQ}{8\beta^2}(B\bar{A} - A\bar{B})\sin 2\beta\eta$$

$$-R\,B\,\bar{B}\left(\frac{\cosh\lambda\eta}{\lambda^2} + \frac{\cosh\bar{\lambda}\eta}{\bar{\lambda}^2}\right)$$

$$\left.\left. -R\left(\frac{A\bar{B}}{\lambda^2}\sinh\lambda\eta + \frac{B\bar{A}}{\bar{\lambda}^2}\sinh\bar{\lambda}\eta\right) + \frac{1}{2}RB\bar{B}\eta^2\right\}\right], \tag{53}$$

where,

$$A = \frac{1}{\lambda\sinh\lambda}\left[\frac{M^2}{1 - im} + 2iK^2\cosh\lambda\right],$$

$$\bar{A} = \frac{1}{\lambda\sinh\lambda}\left[\frac{M^2}{1 + im} - 2iK^2\cosh\lambda\right],$$

$$B = -\frac{2iK^2}{\lambda},\ \bar{B} = \frac{2iK^2}{\lambda},$$

$$P = 1 + \frac{M^2}{(1+m^2)\lambda\bar{\lambda}},\ Q = 1 - \frac{M^2}{(1+m^2)\lambda\bar{\lambda}},\ R = \frac{M^2}{(1+m^2)\lambda\bar{\lambda}},$$

$$X = \frac{P}{8\alpha^2}(A\bar{A} + B\bar{B}) - \frac{Q}{8\beta^2}(A\bar{A} - B\bar{B}) - RB\bar{B}\left(\frac{1}{\lambda^2} + \frac{1}{\bar{\lambda}^2}\right),$$

$$Y = \frac{P}{8\alpha^2}(A\bar{A} + B\bar{B})\cosh 2\alpha - \frac{Q}{8\beta^2}(A\bar{A} - B\bar{B})\cos 2\beta$$

$$+\frac{P}{8\alpha^2}(A\bar{B} + B\bar{A})\sinh 2\alpha - \frac{iQ}{8\beta^2}(B\bar{A} - A\bar{B})\sin 2\beta$$

$$-RB\bar{B}\left(\frac{\cosh\lambda}{\lambda^2} + \frac{\cosh\bar{\lambda}}{\bar{\lambda}^2}\right)$$

$$-R\left(\frac{A\bar{B}}{\lambda^2}\sinh\lambda + \frac{B\bar{A}}{\bar{\lambda}^2}\sinh\bar{\lambda}\right) + \frac{1}{2}RB\bar{B}. \tag{54}$$

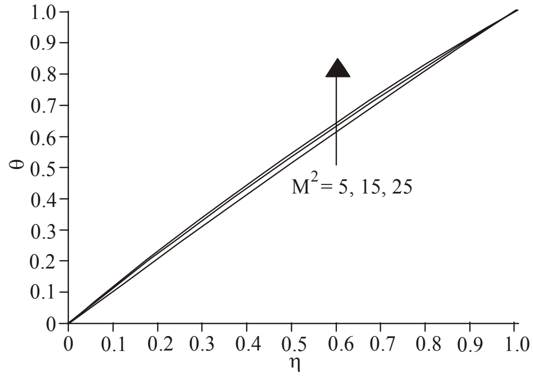

Fig. 13: Temperature variations for M^2 when m = 0.2, K^2 = 20 , Pr = 3.0 and Ec = 0.01

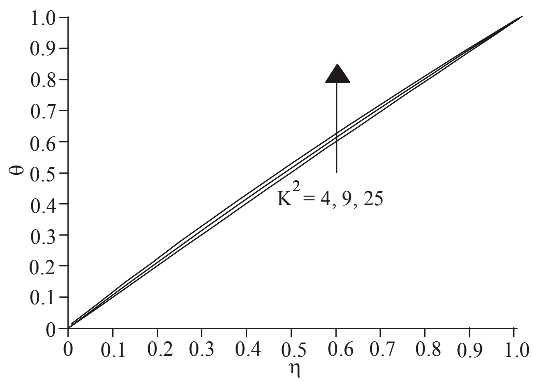

Fig. 14: Temperature variations for K^2 when m = 0.2, M^2 = 10, Pr = 3.0 and Ec = 0.01

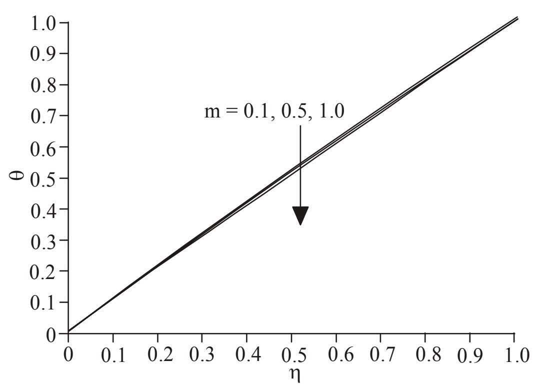

Fig. 15: Temperature variations for m when M^2 = 10, K^2 = 10, Pr = 4.0 and Ec = 0.01

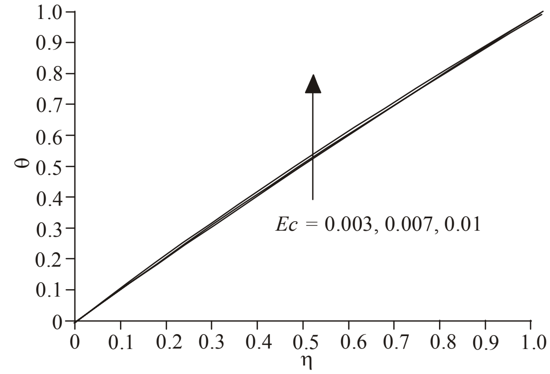

Fig. 16: Temperature variations for Ec when M^2 = 10, K^2 = 10, m = 0.2 and Pr = 3.0

The effects of magnetic parameter M^2, rotation parameter K^2, Hall parameter m and Eckert number Ec on the temperature distribution have been shown in Fig. 13 to 16. It is seen from Fig. 13 to 14 that the fluid temperature $\theta(\eta)$ increases with an increase in either magnetic parameter M^2 or rotation parameter K^2. Figure 15 shows that the fluid temperature $\theta(\eta)$ decreases with an increase in Hall parameter m. It is observed from Fig. 16 that increasing values of Eckert number Ec is to increase the fluid temperature distribution in flow region. This is due to the heat energy stored in the liquid because of the frictional heating.

The rate of heat transfer at the plates $\eta = 0$ and $\eta = 1$ can be obtained from (53) as:

$$\theta'(0) = \left(\frac{d\theta}{d\eta}\right)_{\eta=0} = 1 - PrEc\left[X - Y + \frac{P}{4\alpha}(A\bar{B} + B\bar{A})\right.$$

$$\left. - \frac{iQ}{4\beta}(B\bar{A} - A\bar{B}) - R\left(\frac{A\bar{B}}{\lambda} + \frac{B\bar{A}}{\bar{\lambda}}\right)\right], \qquad (55)$$

$$\theta'(1) = \left(\frac{d\theta}{d\eta}\right)_{\eta=1} = 1 - PrEc\left[X - Y\right.$$

$$+ \frac{P}{4\alpha}(A\bar{A} + B\bar{B})\sinh 2\alpha + \frac{Q}{4\beta}(A\bar{A} - B\bar{B})\sin 2\beta$$

Table 1: Rate of heat transfer at the lower and upper plates when K^2 = 5, Pr = 0.71 and Ec = 0.01

	$\theta'(0)$				$\theta'(1)$			
m\M^2	10	15	20	25	10	15	20	25
0.2	1.011970	1.011215	1.010493	1.009858	0.978506	0.973344	0.969174	0.965590
0.4	1.011080	1.010369	1.009733	1.009186	0.980675	0.975860	0.971880	0.968422
0.6	1.010399	1.009715	1.009137	1.008651	0.982944	0.978539	0.974826	0.971560
0.8	1.009902	1.009223	1.008680	1.008234	0.985082	0.981109	0.977694	0.974661

Table 2: Rate of heat transfer at the lower and upper plates when $M^2 = 10$, $Pr = 0.71$ and $Ec = 0.01$

	$\theta'(0)$				$\theta'(1)$			
m\K^2	4	8	12	16	4	8	12	16
0.2	1.009308	1.020377	1.030215	1.037911	0.979537	0.975244	0.971689	0.969309
0.4	1.008680	1.018611	1.027489	1.034599	0.981446	0.978118	0.975219	0.973169
0.6	1.008198	1.017235	1.025287	1.031823	0.983505	0.980982	0.978672	0.977009
0.8	1.007847	1.016211	1.023605	1.029656	0.985481	0.983581	0.981762	0.980450

Table 3: Rate of heat transfer at the lower and upper plates when $K^2 = 5$, $Pr = 0.71$ and $M^2 = 10$

	$\theta'(0)$				$\theta'(1)$			
m\Ec	0.003	0.005	0.007	0.01	0.003	0.005	0.007	0.01
0.2	1.003591	1.005985	1.008379	1.011970	0.993552	0.989253	0.984954	0.978506
0.4	1.003324	1.005540	1.007756	1.011080	0.994202	0.990337	0.986472	0.980675
0.6	1.003120	1.005200	1.007279	1.010399	0.994883	0.991472	0.988061	0.982944
0.8	1.002971	1.004951	1.006931	1.009902	0.995525	0.992541	0.989558	0.985082

$$+\frac{P}{4\alpha}(A\bar{B}+B\bar{A})\cosh 2\alpha$$

$$-\frac{iQ}{4\beta}(B\bar{A}-A\bar{B})\cos 2\beta - RB\bar{B}\left(\frac{\sinh\lambda}{\lambda}+\frac{\sinh\bar{\lambda}}{\bar{\lambda}}\right)$$

$$\left. -R\left(\frac{A\bar{B}}{\lambda}\cosh\lambda+\frac{B\bar{A}}{\bar{\lambda}}\cosh\bar{\lambda}\right)+RB\bar{B}\right]. \tag{56}$$

where λ is given by (27), A, $\bar{A}$, B, $\bar{B}$, P, Q, R, X and Y are given by (54).

The numerical values of the rate of heat transfer θ′ (0) and θ′ (1) are entered in the Tables 1 to 3 for different values of magnetic parameter M^2, rotation parameter K^2, Eckert number Ec and Hall parameter m. It is seen from Table 1 that the rate of heat transfer decreases both at the lower plate and the upper plate with an increase in magnetic parameter M^2 for fixed value of Hall parameter m. It is observed from Table 2 and 3 that the rate of heat transfer increases at the lower plate (η = 0) while it decreases at the upper plate (η = 1) with an increase in either rotation parameter K^2 or Eckert number Ec for fixed value of Hall parameter m. Further, it is observed from Table 1 to 3 that the rate of heat transfer decreases at the lower plate whereas it increases at the upper plate with an increase in Hall parameter m for fixed values of magnetic parameter M^2, rotation parameter K^2 and Eckert number Ec.

Critical Eckert number at the lower plate η = 0 and at the upper plate η = 1 can be obtained from the Eq. (55) and (56) as:

$$(Ec)_{\eta=0} = Pr^{-1}\left[X - Y + \frac{P}{4\alpha}(A\bar{B}+B\bar{A})\right.$$

$$\left. -\frac{iQ}{4\beta}(B\bar{A}-A\bar{B}) - R\left(\frac{A\bar{B}}{\lambda}+\frac{B\bar{A}}{\bar{\lambda}}\right)\right]^{-1}, \tag{57}$$

$$(Ec)_{\eta=1} = \left[Pr\left\{X - Y + \frac{P}{4\alpha}(A\bar{A}+B\bar{B})\sinh 2\alpha\right.\right.$$

$$+\frac{Q}{4\beta}(A\bar{A}-B\bar{B})\sin 2\beta + \frac{P}{4\alpha}(A\bar{B}+B\bar{A})\cosh 2\alpha$$

$$-\frac{iQ}{4\beta}(B\bar{A}-A\bar{B})\cos 2\beta - RB\bar{B}\left(\frac{\sinh\lambda}{\lambda}+\frac{\sinh\bar{\lambda}}{\bar{\lambda}}\right)$$

$$\left.\left. -R\left(\frac{A\bar{B}}{\lambda}\cosh\lambda+\frac{B\bar{A}}{\bar{\lambda}}\cosh\bar{\lambda}\right)+RB\bar{B}\right\}\right]^{-1}. \tag{58}$$

where λ is given by (27), A, $\bar{A}$, B, $\bar{B}$, P, Q, R, X and Y are given by (54).

The numerical values of the Critical Eckert number $(Ec)_{\eta\text{-o}}$ and $(Ec)_{\eta\text{-}1}$ for several values of M^2, K^2 and m are shown in Table 4 and 5 respectively. It is observed from Table 4 that the absolute value of the Critical Eckert number at the lower plate η = 0 increases while the Critical Eckert number at the upper plate η = 1 decreases on increasing magnetic parameter M^2 for fixed values of Hall parameter m. It is seen from Table 5 that the absolute value of the Critical Eckert number at the lower plate decreases and the Critical Eckert number at the upper plate also decreases with an increase in rotation parameter K^2 for fixed values of Hall parameter m. Further Table 4 and 5 show that the absolute value of the Critical Eckert number at the lower and the upper plates increases with an increase in

Table 4: Critical eckert number at the lower and upper plates when $K^2 = 10$ and Pr = 3

	$-(Ec)_{\eta=0}$				$(Ec)_{\eta=1}$			
$m\backslash M^2$	10	15	20	25	10	15	20	25
0.4	0.101650	0.102098	0.104869	0.108837	0.100929	0.080416	0.069496	0.062548
0.6	0.110266	0.111619	0.114799	0.118956	0.116870	0.092775	0.079662	0.071250
0.8	0.117798	0.120054	0.123664	0.128025	0.136070	0.107653	0.091894	0.081760
1.0	0.124006	0.127167	0.131254	0.135858	0.158140	0.124825	0.106070	0.093836

Table 5: Critical eckert number at the lower and upper plates when $M^2 = 10$ and Pr = 3

	$-(Ec)_{\eta=0}$				$(Ec)_{\eta=1}$			
$m\backslash K^2$	4	8	12	16	4	8	12	16
0.4	0.272672	0.127168	0.086096	0.068403	0.127554	0.108155	0.095505	0.088206
0.6	0.288681	0.137317	0.093592	0.074371	0.143481	0.124447	0.110965	0.102938
0.8	0.301601	0.145994	0.100260	0.079804	0.163008	0.144139	0.129766	0.121058
1.0	0.311266	0.152978	0.105845	0.084457	0.185559	0.166752	0.151275	0.141446

Hall parameter m for fixed values of magnetic parameter M^2 and rotation parameter K^2. It follows from (55) that heat will flow from the lower plate to the fluid if $Ec > (Ec)_{\eta-o}$, while heat will start flowing from the fluid to the lower plate if $Ec < (Ec)_{\eta-o}$. Conversely, it follows from (56) that heat will flow from the fluid to the upper plate if $Ec > (Ec)_{\eta=1}$, while heat will start flowing from upper plate to fluid if $Ec < (Ec)_{\eta=1}$. When Eckert number Ec becomes Critical Eckert number then there is no flow of heat either from fluid to the plates or that from plates to fluid.

This reversal of heat flow may be explained on physical grounds. It is observed that in case there is significant viscous dissipation near the plate, the temperature of the fluid near the plate may exceed plate temperature and for this reason heat will flow from the fluid to the plate even if plate temperature is higher than the ambient temperature. It is noted that in our heat transfer analysis Eq. (48) we have considered the effects of both viscous dissipation and Joule dissipation into account and hence there is a strong reason for the flow of heat from the fluid to the plates under certain conditions.

CONCLUSION

Hall effects on MHD Couette flow between infinite horizontal parallel plates in a rotating system under boundary layer approximation have been studied. The magnetic field has retarding influence on the velocity field as well as the induced magnetic field. Rotation has accelerating influence on the velocity field as well as the induced magnetic field. Hall parameter *m* tends to accelerate the primary fluid flow and to decelerate the secondary flow. On the other hand, it has retarding influence on primary magnetic field and accelerating influence on secondary magnetic field. The fluid temperature increases with an increase in either magnetic parameter M^2 or rotation parameter K^2 or Eckert number Ec while it decreases on increasing Hall parameter m. In the lower plate the primary and the secondary shear stresses decrease with an increase in M^2 whereas they increase on increasing K^2. Further, the rate of heat transfer at the lower plate decreases whereas the rate of heat transfer at the upper plate increases with an increase in Hall parameter m. There exists a single-deck boundary layer in the region near the stationary plate for large values of M^2 and K^2. The boundary layer thickness first decreases, reaches a minimum and then increases with an increase in Hall parameter.

ACKNOWLEDGMENT

We are highly gratified to the reviewers for their valuable comments on this study, which helped us in improving the standard of this study.

REFERENCES

Alpher, R.A., 1961. Heat transfer in magnetohydro-dynamic flow between parallel plates. Int. J. Heat Mass Transfer, 3: 108.

Cowling, T.G., 1957. Magnetohydrodynamics. Intersscience, New York, pp: 101.

Cramer, K. and S. Pai, 1973. Magnetofluid Dynamics for Engineers and Applied Physicists. McGraw-Hill, New York.

Das, B.K., M. Guria and R.N. Jana, 2008. Unsteady couette flow in rotating system. Meccanica, 43: 517.

Das, S., B.C. Sarkar and R.N. Jana, 2011. Hall effects on MHD couette flow in rotating system. Int. J. Com. Appl., 35(13): 22-30.

Ghosh, S.K., 2002. Effects of Hall current on MHD couette flow in a rotating system with arbitrary magnetic field. Czech. J. Phys., 52(1): 51-63.

Gupta, A.S., 1972. Heat transfer in hydromagnetic couette flow with Hall effects. Math. Student, 40: 103-106.

Hartmann, J. and F. Lazarus, 1937. Kgl. Danske Videnskab. Selskab. Mat. Fys. Medd., 15: 6-7.
Jana, R.N., N. Datta and B.S. Mazumder, 1977. Magnetohydrodynamic Couette flow and heat transfer in a rotating system. J. Phys. Soc. Japan, 42: 1034-1039.
Mandal, G., K.K. Mandal and G. Choudhury, 1982. On combined effects of Coriolis force and Hall current on steady MHD Couette flow and heat transfer. J. Phys. Soc. Japan, 51: 2010-2015.
Seth, G.S. and M.K. Maiti, 1982. MHD Couette flow and heat transfer in a rotating system. Ind. J. Pure Appl. Math., 13: 931-945.
Seth, G.S. and N. Ahmad, 1985. Effects of Hall current on MHD Couette flow and heat transfer in a rotating system. J. ISTAM, 30: 177-188.
Seth, G.S., R. Nandkeolyar and M.S. Ansari, 2009. Hall effects on oscillatory hydromagnetic couette flow in a rotating system. Int. J. Acad. Res., 1: 6.
Seth, G.S., S.M. Hussain and J.K. Singh, 2011. MHD couette flow of class-II in a rotating system. Appl. Math. Bioinformatics, 1(1): 31-54.
Seth, G.S., R. Nandkeolyar, N. Mahto and S.K. Singh, 2009. MHD couette flow in a rotating system in the presence of inclined magnetic field. Appl. Math. Sci., 3(59): 2919-2932.
Soundalgekar, V.M., G.A. Dessai and A.S. Gupta, 1974. Hall effects on generalized MHD couete flow with heat transfer. Bull. De La Classe DES Sci., 60: 332-345.
Sutton, G.W. and A. Sherman, 1965. Engineering Magnetohydrodynamics. McGraw-Hill, New York.
Tao, L.N., 1960. Magnetohydrodynamic effects on the formation of couette flow. J. Aerospace Sci., 27: 334.